Journal of Pharmaceutical and Biomedical Analysis 56 (2011) 560–568

Contents lists available at ScienceDirect

Journal of Pharmaceutical and Biomedical Analysis

journal homepage: www.elsevier.com/locate/jpba

Identification and characterization of stressed degradation products of prulifloxacin using LC–ESI-MS/Q-TOF, MS^n experiments: Development of a validated specific stability-indicating LC–MS method

B. Raju [a], M. Ramesh [a], R. Srinivas [a,*], S. Satyanarayana Raju [b], Y. Venkateswarlu [b]

[a] National Centre for Mass Spectrometry, Indian Institute of Chemical Technology, Hyderabad 500 607, India
[b] Division of Organic Chemistry-I, Indian Institute of Chemical Technology, Hyderabad 500 607, India

ARTICLE INFO

Article history:
Received 9 March 2011
Received in revised form 22 June 2011
Accepted 25 June 2011
Available online 2 July 2011

Keywords:
Prulifloxacin
LC–ESI-MS
Tandem mass spectrometry
Degradation products
Accurate mass measurements

ABSTRACT

A rapid, specific and novel gradient LC–MS method has been developed and validated for the identification and characterization of stressed degradation products (DPs) of prulifloxacin (PF) using liquid chromatography combined with quadrupole time-of-flight electrospray ionization tandem mass spectrometry (LC/Q–TOF–ESI-MS/MS). PF was subjected to hydrolytic (acidic, alkaline and neutral), oxidation, photolytic and thermal stress, as per ICH guidelines Q1A (R2). The drug showed extensive degradation in hydrolytic and oxidative, while it was stable to thermal and photolytic stress conditions. In total, 13 DPs were formed and the chromatographic separation of drug and its DPs was achieved on a C-18 column (4.6 × 250 mm, 5 μm) using gradient elution method. All the DPs have been identified and characterized using MS^n experiments and accurate mass measurements. The LC–MS method was validated with respect to specificity, linearity, accuracy, precision and robustness.

1. Introduction

Most of the drugs undergo physicochemical degradation upon storage and it is essential to characterize the degradation products (DPs) in drug discovery and development process. Therefore, it is required to carry out stability testing studies of a drug under various temperature and humidity conditions and report the DPs as per the guidelines of International Conference on Harmonization (ICH) and other international agencies [1–4]. LC/MS combined with electrospray ionization technique has been well established for identification and characterization of DPs [5–11].

Prulifloxacin (PF) is a new thiazeto-quinolone antibacterial agent with a broad-spectrum in vitro activity against various Gram-negative and Gram-positive bacteria and reported to act directly on bacterial DNA gyrase inhibiting cell reproduction that leads to cell death [12]. It exhibits concentration dependent killing and has a persistent post-antibiotic effect [13]. According to IUPAC nomenclature, PF is 6-fluoro-1-methyl-7-[4-[(5-methyl-2-oxo-1,3-dioxol-4-yl)methyl]-1-piperazinyl]-4-oxo-1H,4H-[1,3]thiazeto[3,2-a] quinoline-3-carboxylic acid (Scheme 1). As it consists a quinolone skeleton with four-membered ring on 1 and 2 positions including a sulfur atom, the antibacterial activity is enhanced. The oxodioxolenylmethyl moiety in the 7-piperazine ring helps improve its oral absorption. Following oral administration, it is absorbed in the upper small intestine and metabolized to ulifloxacin by enzyme esterases [14–16]. It has been reported that rats exhibit maximum concentration of active metabolite ulifloxacin in tissues within 1 h [17].

Lingli et al. [18] and Wang et al. [19] have reported a method for quantification of ulifloxacin in human plasma by capillary zone electrophoresis and lanthanide sensitized chemiluminescences of flow-injection. Zhongju et al. [20] also reported a capillary electrophoresis chemiluminescences method for determining norfloxacin and PF in tablet and in urine. A stability-indicating HPLC method for the quantitative determination of PF in pharmaceutical dosage forms was developed and applied to the assay of PF in tablet and bulk form [21]. As there are no reports available on the degradation behavior, identification and characterization of DPs of PF formed under various stress conditions, we have carried out a detailed study on stability indicating LC–MS/MS method for PF.

2. Experimental

2.1. Chemicals and reagents

PF was a gift sample from local manufacturing unit, Hyderabad, India. HPLC grade methanol and acetonitrile used in the present study were purchased from Merck, (Mumbai, India), and used with-

* Corresponding author. Tel.: +91 40 27193122; fax: +91 40 27193156.
E-mail addresses: srini@iict.res.in, sragampeta@yahoo.co.in (R. Srinivas).

0731-7085/$ – see front matter © 2011 Elsevier B.V. All rights reserved.
doi:10.1016/j.jpba.2011.06.021

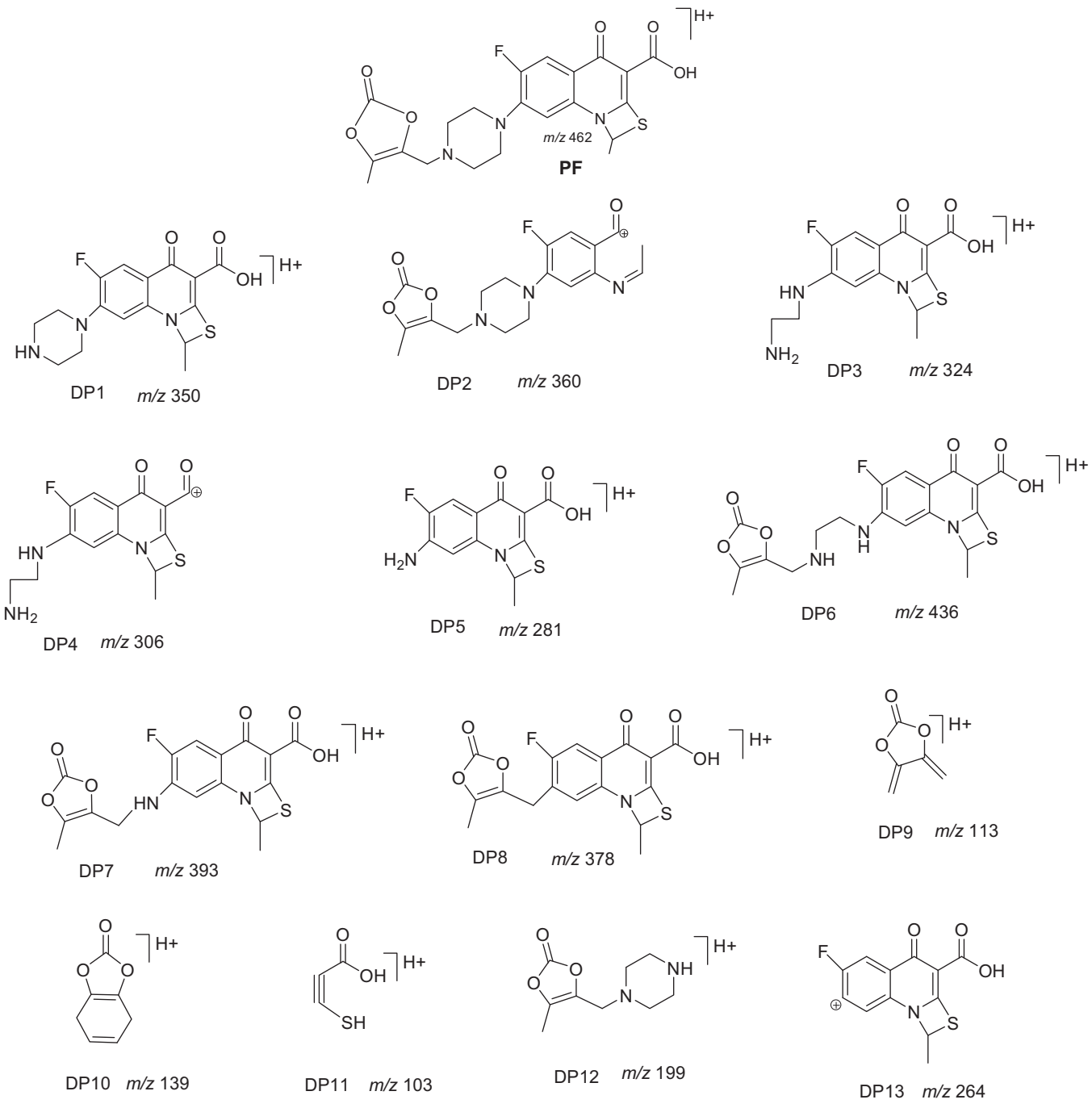

Scheme 1. Proposed structures of DPs formed under various stress conditions.

out further purification. Water was purified by using a Millipore Milli-Q plus purification system. Analytical reagent grade formic acid, hydrochloric acid, sodium hydroxide, and hydrogen peroxide used in the present study were purchased from S.D Fine chemicals (Mumbai, India).

2.2. Instrumentation

2.2.1. High performance liquid chromatography (HPLC)

The analyses were performed on an Agilent 1200 series HPLC instrument (Agilent Technologies, USA) equipped with a Quaternary pump (G1311A, USA), a de-gasser (G1322A, USA), a diode-array-detector (G1315D, USA), an Autosampler (G1329A, USA), a column compartment (G1316A, USA) and Milli Q system (Millipore Corp., Bedford, MA, USA). The samples were separated on a Waters symmetry C-18 column (4.6×250 mm, 5 μm). The mobile phase consists of 0.2% formic acid (solvent A), acetonitrile (solvent B), and methanol (solvent C). A gradient elution program is described in the context of optimization of LC–MS conditions. The mobile phase flow rate is 1.0 mL/min. The column temperature is maintained at 25 °C and the analysis is carried out at the detection wavelength of 273 nm.

2.2.2. Mass spectrometry

For LC–MS analysis, an Agilent 1200 series HPLC instrument (Agilent Technologies, USA) coupled to a quadrupole time-of-flight (Q-TOF) mass spectrometer (Q-TOF LC/MS 6510 series classic G6510A, Agilent Technologies, USA) equipped with an ESI source.

The data acquisition was under the control of Mass Hunter workstation software. A splitter was placed before the ESI source, allowing entry of only 35% of the eluent. The typical operating source conditions for MS scan of PF in positive ESI mode were optimized as follows; the fragmentor voltage was set at, 80 V; the capillary at, 3000–3500 V; the skimmer at, 60 V; nitrogen was used as the drying (300 °C; 9 L/min) and nebulizing (45 psi) gas. For collision-induced dissociation (CID) experiments, keeping MS^1 static, the precursor ion of interest was selected using the quadrupole analyzer and the product ions were analyzed using a time-of-flight (TOF) analyzer. Ultra high pure nitrogen was used as collision gas, and the pressure in the collision cell was maintained at 18 Torr. All the spectra were recorded under identical experimental conditions, and are average of 20–25 scans.

MS^n experiments were performed using a quadrupole ion trap mass spectrometer (Thermo Finnigan, San Jose, CA, USA), equipped with an electrospray source. The data acquisition was under the control of Xcalibur software (Thermo Finnigan). The typical source conditions were: spray voltage, 5 kV; capillary voltage, 15–20 V; heated capillary temperature, 200 °C; tube lens offset voltage, 20 V; sheath gas (N_2) pressure, 20 psi; and helium was used as damping gas. For the ion-trap analyzer, the automatic gain control (AGC) setting were 2×10^7 counts for a full-scan mass spectrum and 2×10^7 counts for a full product ion mass spectrum with a maximum ion injection time of 200 ms. In the full-scan MS^2 mode, the precursor ion of interest was first isolated by applying an appropriate wave form across the end-cap electrodes of the ion-trap to resonantly eject all trapped ions, except those ions of m/z ratio of interest. The isolated ions were then subjected to a supplementary ac signal to resonantly excite them and so cause collision induced dissociation (CID). The collision energies used were 15–37 eV. The excitation time used was 30 ms. All the spectra were recorded under identical experimental conditions, and average of 20–25 scans.

2.3. Stressed degradation studies

Stress degradation studies were carried out on the bulk drug (PF) to provide the ability of the stability-indicating property and specificity of the proposed method as per ICH guidelines Q1A (R2).

Amount of about 10.0 mg of drug was subjected to stress degradation under acidic, basic and neutral conditions by refluxing with 10.0 mL of 0.1 N HCl, 1 N NaOH, and H_2O at 80 °C for 24 h, 72 h, and 72 h, respectively. The oxidative degradation of the drug was carried out using 3%, 6%, 30% H_2O_2 for about 7 days. The PF was spread about 1.0 mm thickness in a Petri dish and kept at 100 °C for 3 days for thermal stress. The drug was exposed to UV light at 320 nm for 10 days in solid as well as solution form (acetonitrile:water, 50:50) for photolytic stress. After the completion of stress degradation, all the samples were kept in refrigerator at 5 °C.

2.4. Sample preparation for HPLC and LC–MS analysis

The stressed samples of acid and base hydrolysis were neutralized with NaOH and HCl, respectively. All the stressed samples (hydrolytic, oxidative, thermal, and photolytic stress) are diluted with mobile phase to 10 times. All these prepared samples are filtered through 0.22 μm membrane filter before HPLC and LC–MS analysis.

3. Results and discussion

3.1. Optimization of LC–MS conditions

The main aim of this work is to separate PF and its DPs. A Waters symmetry C-18 column (250 × 4.6 mm, 5 μm) was found to be suitable for this analysis after tried with different columns. During the optimization process on this column, several conditions with various mobile phases like methanol/water and acetonitrile/water in different proportions were tried in an isocratic mode. Neither methanol nor acetonitrile gave sufficient resolution alone. The resolution of PF and its DPs was influenced by the concentration of ACN in the mobile phase. The peaks were merged when the ACN concentration was increased. While there was improvement in the resolution with the decrease in the percentage of organic modifier, addition of MeOH to the mobile phase improves resolution between the peaks to a good extent. Mixture of water:acetonitrile:methanol (A:B:C) in different proportions was used. Different additives were tried in water (solvent A) like formic acid, acetic acid, and trifluoroacetic acid with various concentrations was considered. At higher concentration of acid, ion suppression was observed when subjected to ESI and at lower concentration, separation of drug and its DPs was not optimum. A concentration of 0.2% formic acid as mobile phase was found to be suitable. During this optimization process, it is observed that, peak area is increasing with the increase in the additive concentration in the mobile phase. Finally we achieved a good resolution of peaks with acceptable shape with the mobile phase consisting of 0.2% formic acid (A), acetonitrile (B) and methanol (C) in a gradient elution program. The solvent program was set as follows: (T_{min}/% solution of B): $_{0–0}$/5, $_{0–9}$/5, $_{9–15}$/75, $_{15–20}$/5, $_{20–25}$/5 and throughout the run solvent C remains 15%. The flow rate 1.0 mL/min, column temperature 25 °C and wavelength of 273 nm were found to be suitable to achieve the separation of PF and its DPs and the method was found to be specific.

The ESI source conditions were also optimized to obtain a good signal and high sensitivity. The conditions like drying gas flow, nebulizing gas flow, drying gas temperature, capillary voltage, spray voltage and skimmer voltage are optimized to maximize the ionization in the source, response and sensitivity even at a very low concentration were optimized to identify and characterize the DPs. Validation of the optimized LC–MS method was done with respect to various parameters outlined in ICH guidelines Q1A (R2) [1–4] and extended to LC–MS/MS.

3.2. Method validation

3.2.1. Specificity

Specificity is the ability of the analytical method to measure the analyte concentration accurately in presence of all potential DPs. The specificity was determined by subjecting PF to stress degradation under various conditions. All the DPs were well separated (Fig. 1), peak purity assessment was carried out on the stressed samples of PF by using diode-array-detector and the specificity was also demonstrated by subjecting all the degradation samples to LC–MS analysis using the same method. The mass detector also showed an excellent mass purity for PF and every DP which unambiguously proves the specificity of the method.

3.2.2. Linearity

Linearity test solutions were prepared from stock solution at six concentration levels of analyte (0.5, 1.0, 2.0, 5.0, 10.0, and 20.0 ng/mL). The peak area versus concentration data is performed by least squares linear regression analysis. The calibration curve was drawn by plotting PF average area for triplicate injections and the concentration expressed as a percentage. Linearity was checked over the same concentration range for three consecutive days. Good linearity was observed in the concentration range from 0.5 to 20.0 ng/mL of PF. The data is subjected to statistical analysis using a linear regression model; the linear regression equation and correlation coefficient (r^2) were $y = 357{,}431x + 140{,}311$, and 0.9996, respectively. These results indicate a good linearity. The LOD and LOQ for PF were estimated at a signal-to-noise ratio of 3:1 and

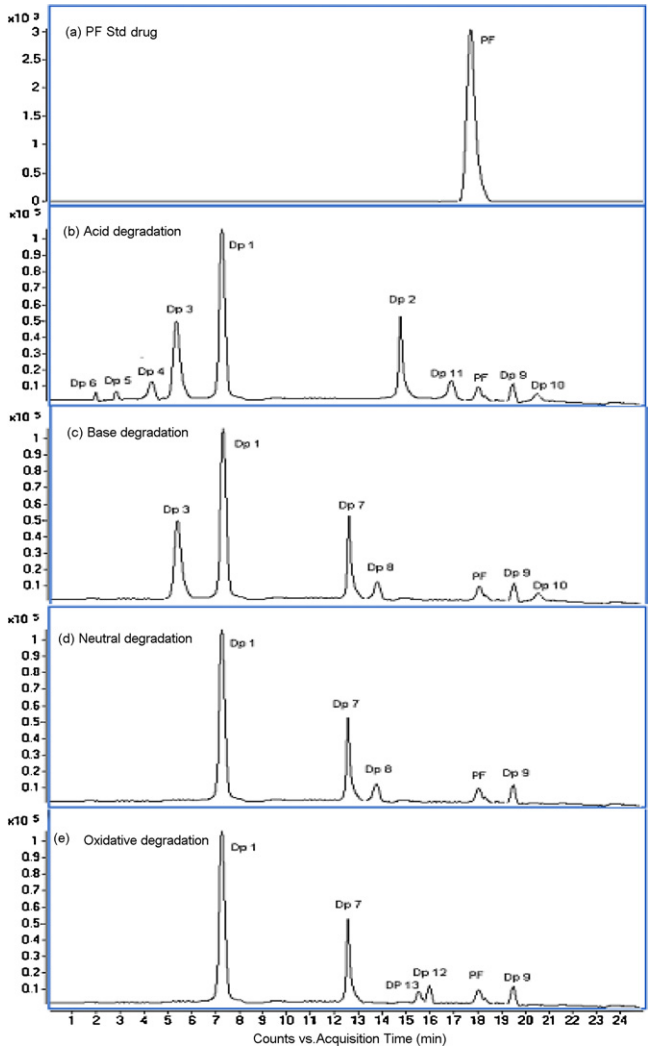

Fig. 1. (a) LC–ESI-MS–TIC of PF std, (b) LC–ESI-MS–TIC of acid degradation products, (c) LC–ESI-MS–TIC of base degradation products, (d) LC–ESI-MS–TIC of neutral degradation products, and (e) LC–ESI-MS–TIC of oxidative degradation products.

10:1, respectively. The LOD and LOQ were 0.02 ng/mL, 0.06 ng/mL, respectively.

3.2.3. Accuracy and precision

Intra- and inter-day precision and accuracy was assessed using three quality control samples. Three replicates were analyzed everyday to determine the intra-day accuracy and precision. The procedure was repeated three times over 3 days in order to determine the inter-day accuracy and precision. Good precision and accuracy was observed. The precision and accuracy of the method is well within the limits. The % RSD for intra and inter day precision was <0.15% and <0.20%, respectively. The percentage of added drug obtained from the difference between peak area of fortified and unfortified degraded samples of PF was found to be 99.2–101.5%.

3.2.4. Robustness

To determine the robustness of the method, experimental conditions were purposely altered. The flow rate of the mobile phase is 1.0 mL/min. We studied the effect of flow rate on the resolution by changing from 0.9 to 1.1 mL/min while the other mobile phase components were held constant. The effect of column temperature on resolution was also studied at 20 °C and 30 °C, instead of 25 °C while the other mobile phase components were held constant. As no significant changes in assay value were observed by changing these chromatographic conditions (flow rate and column temperature), confirms that the robustness of the method.

3.3. Degradation behavior

The optimized LC–MS method is applicable to identify the DPs and the LC–ESI-MS total ion chromatograms (TIC) obtained for PF under various stress conditions are given in Fig. 1. Unreacted drug solution showed only one major peak, which is depicted in Fig. 1a. A total of 13 DPs were identified and characterized by tandem mass spectrometric analysis (LC–ESI-MS/MS). The proposed structures of DPs and their elemental compositions are given in Scheme 1 and Table 1, respectively.

3.3.1. Acidic conditions

The drug degraded extensively, but gradually, with time over 24 h on heating at 80 °C in 0.1 N HCl, forming, in total 9 DPs (DP1–DP6 and DP9–DP11). The drug was found to be degraded in the acidic medium within 3 h to form the major degradation product DP1, and the other DPs, DP2 and DP3. After 6 h DP4, DP5, DP6, and after 12 h, DP9, DP10, and DP11 were formed. No additional DPs were formed after 72 h, indicating that the drug degraded completely within 24 h. The LC–ESI-MS-TIC of acid DPs is given in Fig. 1b. No additional DPs were formed even though the study was extended up to 72 h with 1 N HCl.

3.3.2. Basic conditions

No DPs were formed under basic conditions within 24 h. After 48 h two DPs, DP1 and DP3 were formed. When this study was extended up to 72 h, other 4 DPs, DP7, DP8, DP9 and DP10 were formed. The LC–ESI-MS-TIC of base DPs is given in Fig. 1c. No additional DPs were formed even though the study was extended up to 72 h with 1 N NaOH.

3.3.3. Neutral conditions

No DPs were formed under neutral conditions within 48 h. When the study was extended up to 72 h, four DPs, DP1, DP7, DP8 and DP9 were formed. The LC–ESI-MS-TIC of neutral DPs is given in Fig. 1d.

3.3.4. Oxidative conditions

Under oxidative conditions the drug is oxidized using 3% H_2O_2, 6% H_2O_2, and 30% H_2O_2 for 7 days. It is observed that 3% and 6% H_2O_2 did not affect the drug even after 7 days, whereas 30% H_2O_2 could degrade the drug after 7 days at ambient temperature. Under these conditions four DPs, DP1, DP7, DP9, DP12 and DP13 were formed. The LC–ESI-MS-TIC of oxidative DPs is given in Fig. 1e.

3.3.5. Thermal and photolytic conditions

The drug was found to be stable in solid as well as in solution forms (acetonitrile:water, 50:50) under UV light. For thermal solid stress, the drug was kept at 100 °C in oven for 3 days. The drug was not degraded even though the study was extended up to 3 days under thermal conditions.

3.4. Characterization of PF and its DPs by LC–MS/MS, MS^n experiments

3.4.1. MS/MS CID of PF

The positive ion ESI-MS of PF shows abundant $[M+H]^+$ and low abundance $[M+Na]^+$ ions. The LC–ESI-MS/MS spectrum of $[M+H]^+$ ions (*m/z* 462) of PF shows abundant product ions at *m/z* 444 (loss of H_2O), *m/z* 360 (loss of 3-mercaptopropiolic

Table 1
Elemental compositions of PF and its DPs (DP1–DP13).

PF&DPs	Rt (min)	Proposed formula	Observed mass (Da)	Calculated mass (Da)	Error (ppm)	Proposed neutral loss	MS/MS fragment ions
PF	18.2	$C_{21}H_{21}N_3O_6FS$	462.1135	462.1130	−1.25	–	444, 418, 400, 360, 350, 332, 306, 289, 263, 248, 113.
DP1	7.3	$C_{16}H_{17}N_3O_3FS$	350.0983	350.0969	−3.92	$C_5H_4O_3$	332, 306, 289, 263, 248, 222, 205
DP2	14.9	$C_{18}H_{19}N_3O_4F$	360.1365	360.1354	−3.85	$C_3H_2SO_2$	334, 316, 246, 219, 205, 191, 177, 164, 149, 138, 123, 110, 95
DP3	5.5	$C_{14}H_{15}N_3O_3FS$	324.0800	324.0812	3.95	$C_7H_6O_3$	306, 289, 263, 235, 222, 205, 179, 164.
DP4	4.5	$C_{14}H_{13}N_3O_2FS$	306.0712	306.0707	−2.98	$C_7H_8O_4$	289, 263, 248, 222, 204, 176, 148.
DP5	2.9	$C_{12}H_{10}N_2O_3FS$	281.0396	281.0391	−1.89	$C_9H_{11}NO_3$	263, 237, 235, 201, 179, 176, 148, 130, 122.
DP6	16.9	$C_{19}H_{19}N_3O_6FS$	436.0971	436.0973	0.98	C_2H_2	418, 362, 350, 344, 334, 332, 318, 306, 289, 263, 248.
DP7	12.5	$C_{17}H_{14}N_2O_6FS$	393.0562	393.0551	−2.64	C_4H_7N	375, 331, 291, 250, 149, 113
DP8	13.8	$C_{17}H_{13}NO_6FS$	378.0449	378.0442	−0.62	$C_4H_8N_2$	360, 332, 276, 240, 172, 157, 103, 91.
DP9	19.6	$C_5H_5O_3$	113.0234	113.0233	−0.61	$C_{16}H_{16}N_3O_3FS$	–
DP10	20.5	$C_7H_7O_3$	139.0391	139.0390	−0.78	$C_{14}H_{14}N_3O_3FS$	–
DP11	2.0	$C_3H_3SO_2$	103.9914	103.9927	2.99	$C_{18}H_{18}N_3O_4F$	–
DP12	15.5	$C_9H_{15}N_2O_3$	199.1064	199.1077	4.87	$C_{12}H_6NO_3FS$	173, 156, 155, 113, 85.
DP13	16.0	$C_{12}H_7NO_3FS$	264.0138	264.0125	−4.89	$C_9H_{14}N_2O_3$	162, 134, 121.

acid, 102 Da), and low abundance product ions at *m/z* 350 (loss of 4,5-dimethylene-1,3-dioxolan-2-one, 112 Da), *m/z* 332 (loss of H_2O from *m/z* 350), *m/z* 306 (loss of C_2H_2 from *m/z* 332), *m/z* 418 (loss of CO_2), *m/z* 400 (loss of CO_2 from *m/z* 444), *m/z* 289 (loss of NH_3 from *m/z* 306), *m/z* 263 (loss of C_2H_2 from *m/z* 289), *m/z* 248 (loss of CH_3CN from *m/z* 289), and *m/z* 113 (protonated 4,5-dimethylene-1,3-dioxolan-2-one) (Scheme 2). All these fragmentation pathways have been confirmed by MS^n experiments and accurate mass measurements (Table 2).

3.4.2. MS/MS CID of DPs

All the DPs, DP1–DP13 were eluted within 21 min on C-18 column. The retention times (Rt) of these DPs are given in Table 1. The proposed structures and elemental composition of all the DPs are shown in Scheme 1 and Table 1. To characterize the DPs, we have

Table 2
Elemental compositions of daughter ions of PF (*m/z* 462), DP1 (*m/z* 350), DP2 (*m/z* 360), DP3 (*m/z* 324), and DP4 (*m/z* 306).

	Proposed formula	Observed mass (Da)	Calculated mass (Da)	Error(ppm)	Proposed neutral loss
PF	$C_{21}H_{21}N_3O_6FS$	462.1135	462.1130	−1.25	–
	$C_{21}H_{19}N_3O_5FS$	444.1021	444.1024	2.98	H_2O
	$C_{20}H_{21}N_3O_4FS$	418.1271	418.1231	−3.78	CO_2
	$C_{20}H_{19}N_3O_3FS$	400.1121	400.1126	2.99	CO_2
	$C_{16}H_{17}N_3O_3FS$	350.0983	350.0969	−3.92	$C_5H_4O_3$
	$C_{16}H_{15}N_3O_2FS$	332.0866	332.0864	−0.73	H_2O
	$C_{14}H_{13}N_3O_2FS$	306.0712	306.0707	−2.98	C_2H_2
	$C_{14}H_{10}N_2O_2FS$	289.0441	289.0442	0.16	NH_3
	$C_{12}H_8\ N_2O_2FS$	263.0376	263.0285	4.89	C_2H_2
	$C_{12}H_7NO_2FS$	248.1173	248.1194	3.98	CH_3CN
DP1	$C_5H_5O_3$	113.0234	113.0233	−0.61	$C_{16}H_{16}N_3O_3FS$
	$C_{11}H_{13}N_3OF$	222.1038	222.1037	−1.02	C_2H_2
	$C_{11}H_{10}N_2OF$	205.0777	205.0772	−4.89	CH_3CN
DP2	$C_{18}H_{19}N_3O_4F$	360.1365	360.1354	−3.85	$C_3H_2O_2S$
	$C_{16}H_{17}N_3O_4F$	334.1189	334.1198	3.89	C_2H_2
	$C_{17}H_{19}N_3O_2F$	316.1462	316.1456	−5.89	CO_2
	$C_{13}H_{13}N_3OF$	246.1039	246.1037	−0.87	$C_5H_6O_3$
	$C_{12}H_{12}N_2OF$	219.0929	219.0928	−0.36	HCN
	$C_{10}H_8N_2OF$	191.0602	191.0615	3.25	C_2H_4
	$C_{11}H_{10}N_2OF$	205.0787	205.0772	−4.89	CH_3CN
	$C_{10}H_{10}N_2F$	177.0834	177.0823	−5.21	CO
	C_9H_7NOF	164.0562	164.0506	−8.36	CH_3CN
	$C_8H_6N_2F$	149.0519	149.0510	−0.78	C_2H_4
	$C_6H_4N_2F$	123.0354	123.0353	−0.21	C_2H_2
	C_6H_4F	95.0291	95.0292	0.35	N_2
	C_6H_5NF	110.0471	110.0401	−8.21	CO
	C_7H_5NOF	138.0361	138.0350	−2.58	C_2H_2
DP3	$C_{14}H_{15}N_3O_3FS$	324.0800	324.0812	3.95	$C_7H_6O_3$
	$C_{11}H_8\ N_2OFS$	235.0346	235.0336	−3.12	CO
	$C_9H_8N_2OF$	179.0166	179.0165	−0.28	C_2H_2
DP4	$C_{10}H_6NO_2S$	204.0134	204.0114	−5.28	C_2HF
	C_9H_6NOS	176.0169	176.0165	−2.93	CO
	C_8H_6NS	148.0217	148.0215	−0.20	CO

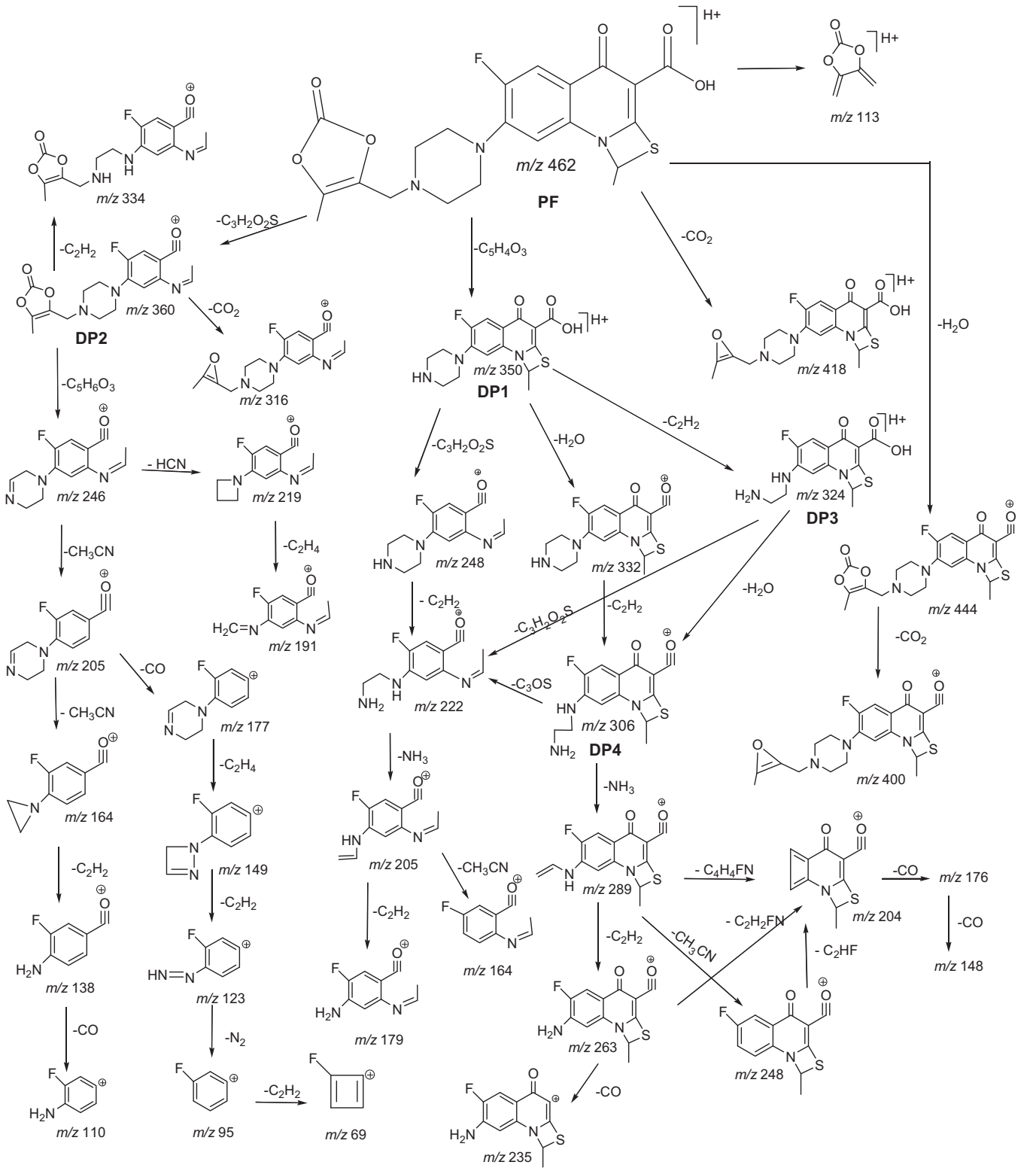

Scheme 2. Proposed fragmentation mechanism for PF, DP1, DP2, DP3, and DP4.

performed online LC–ESI-MS/MS experiments. The elemental composition of all the DPs and their fragment ions were confirmed by accurate mass measurements.

3.4.2.1. DP1 ([M+H]$^+$, m/z 350). The ESI-MS/MS spectrum of [M+H]$^+$ ions (*m*/*z* 350) of DP1, eluting at retention time (Rt) 7.3 min in LC, shows the abundant product ions at *m*/*z* 332 (loss of H_2O), *m*/*z* 306 (loss of C_2H_2 from *m*/*z* 332), and *m*/*z* 248 (loss of 3-mercaptopropiolic acid) (Scheme 2). The spectrum also displays low abundance ions at *m*/*z* 289 (loss of NH_3 from *m*/*z* 306), *m*/*z* 263 (loss of C_2H_2 from *m*/*z* 289), *m*/*z* 222 (loss of C_2H_2 from *m*/*z* 248), and *m*/*z* 205 (loss of NH_3 from *m*/*z* 222). The *m*/*z* 248 ion can also be formed from *m*/*z* 289 by the loss of CH_3CN. These fragmentation pathways have been confirmed by MS^n experiments in an

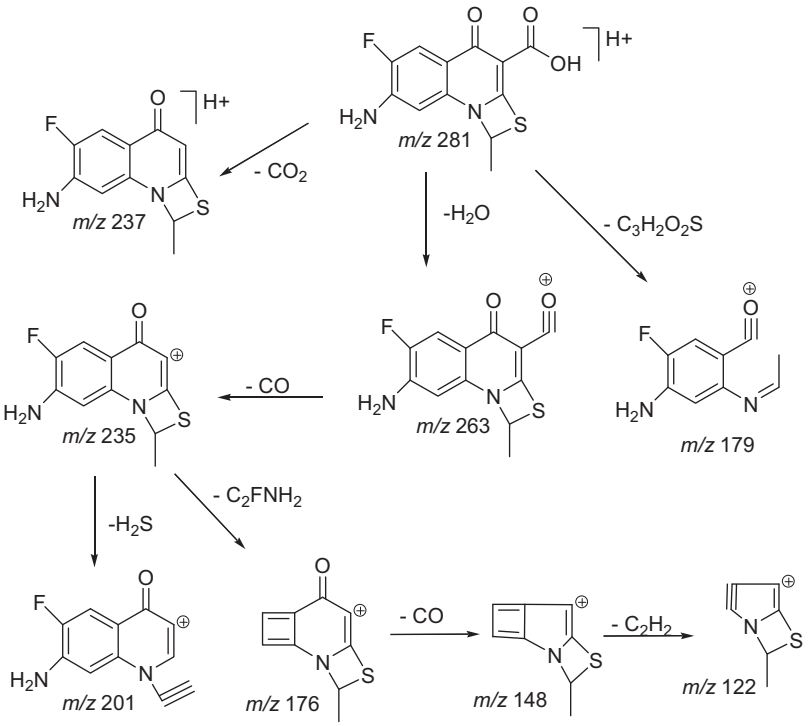

Scheme 3. Proposed fragmentation mechanism for DP5 (*m/z* 281).

ion-trap mass spectrometer. The loss of 3-mercaptopropiolic acid (102 Da), which is also a characteristic fragmentation of the protonated PF, suggests the presence of COOH group and thiazeto ring in the DP1. The formation of fragment ions at *m/z* 306, *m/z* 222, and *m/z* 205, indicate the presence of piperazine ring. The elemental compositions of all the fragment ions have been confirmed by accurate mass measurements (Table 2). Based on the accurate MS/MS spectra and in comparison with previous report [22], DP1 was identified as ulifloxacin (6-fluoro-1-methyl-4-oxo-7-(piperazin-1-yl)-1,4-dihydro-[1,3] thiazetidino[3,2-a] quinoline-3-carboxylic acid) which is a major DP under hydrolytic and oxidative stress conditions.

3.4.2.2. DP2 (m/z 360). The ESI-MS/MS spectrum of $[M+H]^+$ ions (*m/z* 360) of DP2 eluting at Rt 14.9 min displays the abundant product ions at *m/z* 246 (loss of 4,5-dimethyl -1,3-dioxol-2-one, 114 Da), *m/z* 219 (loss of HCN from *m/z* 246), *m/z* 205 (loss of CH_3CN from *m/z* 246), *m/z* 191 (loss of C_2H_4 from *m/z* 219), *m/z* 177 (loss of CO from *m/z* 205), *m/z* 164 (loss of CH_3CN from *m/z* 205), *m/z* 149 (loss of C_2H_4 from *m/z* 177), *m/z* 138 (loss of C_2H_2 from *m/z* 164), and *m/z* 123 (loss of C_2H_2 from *m/z* 149). In addition, the spectrum also shows the low abundance ions at *m/z* 334 (loss of C_2H_2), *m/z* 316 (loss of CO_2), *m/z* 110 (loss of CO from *m/z* 138), and *m/z* 95 (loss of N_2 from *m/z* 123) (Scheme 2, Table 2). The formation of *m/z* 246 ion can be explained by a plausible mechanism involving a migration of 'H' from the carbon bearing 'N-4' of piperazine ring to the $-CH_2$ group of dioxol-2-one ring followed by the loss of 4,5-dimethyl -1,3-dioxol-2-one, (114 Da)) (Scheme 2). The formation of *m/z* 246 ion indicates that the structure of DP2 contains a dioxol-2-one ring. The neutral losses of CH_3CN, C_2H_2, C_2H_4 and N_2 indicate that the structure of DP2 may contain piperazine ring and that piperazine ring is directly attached to aromatic ring. The formation of the ions at *m/z* 177 and *m/z* 110 may indicate that the structure of DP2 contain CO group which is present in the quinolone ring. All these fragmentation pathways have been confirmed by MS^n experiments and accurate mass measurements (Table 2). Therefore, DP2 was identified as (2-(ethylideneamino)-5-fluoro-4-(4-((5-methyl-2-oxo-1,3-dioxol-4-yl)methyl)piperazin-1-yl) phenyl)(oxo)methylium.

3.4.2.3. DP3 ($[M+H]^+$, m/z 324). The ESI-MS/MS spectrum of $[M+H]^+$ ions (*m/z* 324) of DP3 (Rt 5.5 min), shows the product ions at *m/z* 306 (loss of H_2O), *m/z* 289 (loss of NH_3 from *m/z* 306), *m/z* 263 (loss of C_2H_2 from *m/z* 289), *m/z* 235 (loss of CO from *m/z* 263), *m/z* 222 (loss of 3-mercaptopropiolic acid), *m/z* 205 (loss of NH_3 from *m/z* 222), *m/z* 179 (loss of C_2H_2 from *m/z* 205), and *m/z* 164 (loss of CH_3CN from *m/z* 205) (Scheme 2) (Table 2). All these fragmentation pathways have been confirmed by MS^n experiments. Similarly to DP1 and DP2, the loss of 3-mercaptopropiolic acid is indicative of the presence of thiazeto ring and COOH group in DP3. Based on the MS/MS and MS^n experiments combined with elemental composition, the structure of 7-(2-aminoethylamino)-6-fluoro-1-methyl-4-oxo-1,4-dihydro-[1,3]thiazetidino[3,2-a] quinoline-3-carboxylic acid can be ascribed to DP3. The formation of DP3 fragment ion from the protonated PF, through a likely pathway is shown in Scheme 2.

3.4.2.4. DP4 (m/z 306). The ESI-MS/MS spectrum of $[M+H]^+$ ions (*m/z* 306) of DP4 (Rt 4.5 min), shows the product ions at *m/z* 289 (loss of NH_3), *m/z* 263 (loss of C_2H_2 from *m/z* 289), *m/z* 248 (loss of CH_3CN from *m/z* 289), *m/z* 222 (loss of C_3SO), *m/z* 204 (loss of C_4H_4NF from *m/z* 289), *m/z* 176 (loss of CO from *m/z* 204), and *m/z* 148 (loss of CO from *m/z* 176) (Scheme 2) (Table 2). The *m/z* 204 ion can also be formed by the loss of C_2H_2NF, C_2HF from *m/z* 263 and *m/z* 248, respectively. As can be seen from Scheme 2, the fragmentation of DP4 giving rise to all the structure indicative ions, is highly compatible with the proposed structure of (7-(2-aminoethylamino)-6-fluoro-1-methyl-4-oxo-1,4-dihydro-[1,3]thiazetidino[3,2-a]quinolin-3-yl)(oxo)methylium for DP4. All these fragmentation pathways have been confirmed by MS^n experiments and elemental compositions derived from accurate mass measurements (Table 2).

Table 3
Elemental compositions of daughter ions of DP5 (*m/z* 281), DP6 (*m/z* 436), DP7 (*m/z* 393), DP8 (*m/z* 378), DP12 (*m/z* 199) and DP13 (*m/z* 264).

	Proposed formula	Observed mass (Da)	Calculated mass (Da)	Error(ppm)	Proposed neutral loss
DP5	$C_{12}H_{10}N_2O_3FS$	281.0396	281.0391	−1.89	–
	$C_{12}H_8N_2O_2FS$	263.0274	263.0285	+3.58	H_2O
	$C_{11}H_8N_2OFS$	235.0346	235.0336	−3.12	CO
	$C_{11}H_{10}N_2OFS$	237.0487	237.0492	3.28	CO_2
	$C_{11}H_6N_2OF$	201.0447	201.0459	4.58	H_2S
	$C_9H_8N_2OF$	179.0611	179.0615	2.58	$C_3H_2O_2S$
	C_9H_6NOS	176.0158	176.0165	5.24	C_2H_2NF
	C_8H_6NS	148.0221	148.0215	−2.47	CO
	C_6H_4NS	122.0058	122.0059	0.17	C_2H_2
DP6	$C_{19}H_{19}N_3O_6FS$	436.0971	436.0973	0.98	–
	$C_{19}H_{17}N_3O_5FS$	418.0854	418.0867	3.18	H_2O
	$C_{17}H_{17}N_3O_3FS$	362.0966	362.0969	0.12	$C_2H_2O_3$
	$C_{16}H_{17}N_3O_3FS$	350.0965	350.0969	2.81	$C_3H_2O_3$
	$C_{17}H_{15}N_3O_2FS$	344.0858	344.0864	5.21	H_2O
	$C_{16}H_{17}N_3O_4F$	334.1112	334.1198	5.65	$C_3H_2O_2S$
	$C_{17}H_{15}NO_3FS$	332.0762	332.0751	−5.25	N_2H_2
	$C_{16}H_{17}N_3OFS$	318.1054	318.1071	4.87	CO_2
DP7	$C_{14}H_{13}N_3O_2FS$	306.0708	306.0707	−0.12	$C_5H_4O_3$
	$C_{14}H_{10}N_2O_2FS$	289.0387	289.0442	6.25	NH_3
	$C_{12}H_8N_2O_2FS$	263.0265	263.0285	5.21	C_2H_2
	$C_{12}H_7NO_2FS$	248.0168	248.0176	5.93	CH_3CN
	$C_{17}H_{14}N_2O_6FS$	393.0562	393.0551	−2.64	–
	$C_{17}H_{12}N_2O_5FS$	375.0456	375.0445	−3.21	H_2O
	$C_{16}H_{12}N_2O_3FS$	331.0558	331.0547	−3.96	CO_2
	$C_{14}H_{12}N_2O_4F$	291.0757	291.0776	7.36	$C_3H_2O_2S$
	$C_{12}H_9NO_4F$	250.0521	250.0510	−5.12	CH_3CN
DP8	C_5H_5O3	113.0234	113.0233	−0.61	$C_{12}H_9N_2O_3FS$
	$C_{17}H_{13}NO_6FS$	378.0449	378.0442	−0.62	–
	$C_{17}H_{11}NO_5FS$	360.0339	360.0336	−1.36	H_2O
	$C_{16}H_{11}NO_4FS$	332.0372	332.0387	2.83	CO
	$C_{14}H_{11}NO_4F$	276.0661	276.0667	1.22	$C_3H_2O_2S$
	$C_6H_6NO_3S$	172.0059	172.0063	2.21	$C_{11}H_7O_3F$
	$C_7H_6O_3F$	157.0291	157.0295	1.02	$C_{10}H_7NO_3S$
	C_7H_3O	103.0198	103.0178	−5.32	$C_{10}H_{10}NO_5FS$
DP12	$C_9H_{15}N_2O_3$	199.1064	199.1077	4.87	–
	$C_7H_{13}N_2O_3$	173.0935	173.0921	−5.32	C_2H_2
	$C_7H_{10}NO_3$	156.0658	156.0655	−1.96	NH_3
	$C_8H_{15}N_2O$	155.1172	155.1179	1.24	CO_2
	$C_5H_5O_3$	113.0214	113.0233	2.61	$C_4H_{10}N_2$
	$C_4H_9N_2$	85.0783	85.0760	−6.21	$C_5H_6O_3$
DP13	$C_{12}H_7NO_3FS$	264.0138	264.0125	−5.14	–
	C_9H_5NOF	162.0358	162.0350	−2.12	$C_3H_2O_2S$
	C_8H_5NF	134.0411	134.0401	−1.25	CO
	C_7H_2OF	121.0089	121.0084	−2.87	CH_3CN

3.4.2.5. DP5 ([M+H]$^+$, m/z 281). The ESI-MS/MS spectrum of [M+H]$^+$ ions (*m/z* 281) of DP5 (Rt 2.9 min), shows the product ions at *m/z* 263 (loss of H_2O), *m/z* 237 (loss of CO_2), *m/z* 235 (loss of CO from *m/z* 263), *m/z* 201 (loss H_2S from *m/z* 235), *m/z* 179 (loss of 3-mercaptopropiolic acid), *m/z* 176 (loss of C_2H_2NF from *m/z* 235), *m/z* 148 (loss of CO from *m/z* 176), and *m/z* 122 (loss of C_2H_2 from *m/z* 148). All these fragmentation pathways have been confirmed by MS^n experiments and accurate mass measurements (Scheme 3) (Table 3). The observed characteristic fragmentation is highly consistent with the structure 7-amino-6-fluoro-1-methyl-4-oxo-1,4-dihydro-[1,3]thiazetidino[3,2-a] quinoline-3-carboxylic acid, proposed for DP5.

3.4.2.6. DP6 ([M+H]$^+$, m/z 436). The ESI-MS/MS spectrum of [M+H]$^+$ ions (*m/z* 436) of DP6 (Rt 16.9 min), shows the product ions at *m/z* 418 (loss of H_2O), *m/z* 362 (loss of $C_2H_2O_3$), *m/z* 350 (loss of $C_3H_2O_3$), *m/z* 344 (loss of H_2O from *m/z* 362), *m/z* 334 (loss of 3-mercaptopropiolic acid), *m/z* 332 (loss of N_2H_2 from *m/z* 362), *m/z* 318 (loss of CO_2 from *m/z* 362), *m/z* 306 (loss of 4,5-dimethylene-1,3-dioxolan-2-one (112 Da) from *m/z* 418), *m/z* 289 (loss of NH_3 from *m/z* 306), *m/z* 263 (loss of C_2H_2 from *m/z* 289), and *m/z* 248 (loss of CH_3CN from *m/z* 289) (Table 3). All these fragmentation pathways involving characteristic eliminations including that of 4,5-dimethyl-1,3-dioxol-2-one clearly points to the proposed structure 6-fluoro-1-methyl-7-(2-((5-methyl-2-oxo-1,3-dioxol-4-yl) methylamino) ethylamino)-4-oxo-1,4-dihydro-[1,3]thiazetidino [3,2-a] quinoline-3-carboxylic acid for DP6. Similarly to the previous DPs, the elemental compositions of the proposed structures of all the fragment ions have been confirmed by accurate mass measurements.

3.4.2.7. DP7 ([M+H]$^+$, m/z 393). The ESI-MS/MS spectrum of [M+H]$^+$ ions (*m/z* 393) of DP7 (Rt 12.5 min), shows the product ions at *m/z* 375 (loss of H_2O), *m/z* 331 (loss of CO_2 from *m/z* 375), *m/z* 291 (loss of 3-mercaptopropiolic acid), *m/z* 250 (loss of CH_3CN from *m/z* 291), and an important diagnostic ion at *m/z* 113 corresponding to protonated 4,5-dimethylene-1,3-dioxolan-2-one. Based on the fragmentation pattern combined with accurate mass measurements (Table 3), the structure, 6-fluoro-1-methyl-7-((5-methyl-2-oxo-1,3-dioxol-4-yl)methylamino)-4-oxo-1,4-dihydro-[1,3]thiazetidino[3,2-a]quinoline-3-carboxylicacid is proposed for DP7. MS^n experiments have confirmed the fragmentation pathways.

3.4.2.8. DP8 ([M+H]$^+$, m/z 378). The ESI-MS/MS spectrum of [M+H]$^+$ ions (*m/z* 378) of DP8 (Rt 13.8 min), shows the product ions at *m/z* 360 (loss of H_2O), *m/z* 332 (loss of CO from *m/z* 360), *m/z* 276 (loss of 3-mercaptopropiolic acid), *m/z* 172 (protonated 2-methyl-

3-thia-1-aza-bicyclo[2.2.0.]hex-4-ene-5-carboxilic acid), *m/z* 157 (protonated 4-(3-fluoroprop-2-ynyl)-5-methyl-1,3-dioxol-2-one) and *m/z* 103 (1-oxo-1H-cyclopropabenzen-3-ylium). The fragmentation of protonated DP8 is highly compatible with the proposed structure of 6-fluoro-1-methyl-7-((5-methyl-2-oxo-1,3-dioxol-4-yl) methyl)-4-oxo-1,4-dihydro-[1,3]thiazeto [3,2-a] quinoline-3-carboxylic acid for DP8. The fragmentation pathways have been confirmed by MS^n experiments and accurate mass measurements (Table 3).

3.4.2.9. DP9 ($[M+H]^+$, m/z 113), DP10 ($[M+H]^+$, m/z 139) and DP11 ($[M+H]^+$, m/z 103). The formation of DP9 (Rt 19.6 min), corresponding to protonated 4,5-dimethylene-1,3-dioxolan-2-one), can be visualized to be complementary product to DP1, as shown in Scheme 2. The formation of DP10 (Rt 20.5 min; *m/z* 139) may be attributed to the combination of 4,5-dimethylene-1,3-dioxolan-2-one and C_2H_2. Similarly, DP11 (Rt 2.0 min, *m/z* 103) can be assigned the structure of protonated 3-mercaptopropiolic acid, which is eliminated as a neutral species in the formation of majority of the DPs, as discussed previously. Due to the lower *m/z* values of these ions, they were not further selected for MS/MS experiments. The elemental compositions of DP9, DP10, and DP11 have been confirmed by accurate mass measurements (Table 1).

3.4.2.10. DP12 ($[M+H]^+$, m/z 199). The ESI-MS/MS spectrum of $[M+H]^+$ ions (*m/z* 199) of DP12 (Rt 15.5 min), shows the product ions at *m/z* 113 (protonated 4,5-dimethylene-1,3-dioxolan-2-one), *m/z* 173 (loss of C_2H_2), *m/z* 156 (loss of NH_3 from *m/z* 173), *m/z* 155 (loss of CO_2), and *m/z* 85 (protonated 1,2,3,6-tetrahydropyrazine) (Table 3). The formation of *m/z* 113 and *m/z* 85 ions are indicative of the presence of dioxolan-2-one ring and piperazine ring, respectively. Based on accurate MS/MS spectra, DP12 was identified as 4-methyl-5-(piperazin-1-ylmethyl)-1,3-dioxol-2-one.

3.4.2.11. DP13 (m/z 264). The ESI-MS/MS spectrum of $[M+H]^+$ ions (*m/z* 264) of DP13 (Rt 16.0 min), shows the product ions at *m/z* 162 (loss of 3-mercaptopropiolic acid), *m/z* 134 (loss of CO from *m/z* 162) and *m/z* 121 (loss of CH_3CN from *m/z* 162). These fragmentation pathways have been confirmed by MS^n experiments and accurate mass measurements (Table 3). Based on MS/MS fragmentation and accurate measurements, DP13 may be assigned the structure of 3-carboxy-6-fluoro-1-methyl-4-oxo-1,4-dihydro-[1,3]thiazetidino[3,2-a]quinolin-7-ylium.

4. Conclusions

Stress degradation studies on prulifloxacin, carried out according to ICH guidelines, provided information on the degradation behavior of the drug under the conditions of hydrolysis and oxidation. The liquid chromatography method we described here can resolve all DPs from the parent as well as from each other under various stress conditions. The drug showed extensive degradation in hydrolytic and oxidative, while it was stable to thermal and photolytic stress conditions. A total of 13 DPs were characterized with the help of the MS^n experiments combined with accurate mass measurements of fragment ions and precursors.

Acknowledgements

The authors thank Dr. J.S. Yadav, Director, IICT, Hyderabad, for facilities and Dr.V.U.M. Sarma for his cooperation. B.R. thankful to DST for the award of Junior Research Fellowship and M.R. thankful to CSIR, New Delhi, for the award of Senior Research Fellowship.

References

[1] ICH, Stability testing of new drug substances and products Q1A (R2), in: International Conference on Harmonization, IFPMA, Geneva, 2003.
[2] WHO, Draft Stability Testing of Active Pharmaceutical Ingredients and Pharmaceutical Products, World Health Organization, Geneva, 2007.
[3] CPMP, Note for Guidance on Stability Testing: Stability Testing of Existing Active Substances and Related Finished Products, Committee for Proprietary Medicinal Products, EMEA, London, 2002.
[4] TPD, Guidance for Industry Stability Testing of Existing Drug Substances and Products, Therapeutic Products Directorate, Health Canada, Ottawa, ON, 2003.
[5] S. Gorog, The importance and the challenges of impurity profiling in modern pharmaceutical analysis, TrAC 25 (2006) 755–757.
[6] T. Murakami, T. Kawasaki, A. Takemura, N. Fukutsu, N. Kishi, F. Kusu, Identification of degradation products in loxoprofen sodium adhesive tapes by liquid chromatography–mass spectrometry and dynamic pressurized liquid extraction–solid-phase extraction coupled to liquid chromatography–nuclear magnetic resonance spectroscopy, J. Chromatogr. A 1208 (2008) 164–174.
[7] P. Novak, P. Tepes, M. Ilijas, I. Fistric, I. Bratos, A. Avdagic, Z. Hamersak, V.G. Markovic, M. Dumic, LC–NMR and LC–MS identification of an impurity in a novel antifungal drug icofungipen, J. Pharm. Biomed. Anal. 50 (2009) 68–72.
[8] T. Murakami, N. Fukutsu, J. Kondo, T. Kawasaki, Application of liquid chromatography-two-dimensional nuclear magnetic resonance spectroscopy using pre-concentration column trapping and liquid chromatography–mass spectrometry for the identification of degradation products in stressed commercial amlodipine maleate tablets, J. Chromatogr. A 1181 (2008) 67–76.
[9] R.V. Dev, G.S.U. Kiran, B.V. Subbaiah, B.S. Babu, J.M. Babu, P.K. Dubey, K. Vyas, Identification of degradation products in stressed tablets of rabeprazole sodium by HPLC-hyphenated techniques, Magn. Reson. Chem. 47 (2009) 443–448.
[10] R.P. Shah, V. Kumar, S. Singh, Liquid chromatography/mass spectrometric studies on atorvastatin and its stress degradation products, Rapid Commun. Mass Spectrom. 22 (2008) 613–622.
[11] Z. Ying liu, H. Hai Zhang, X. Jun Chen, X. Ni Zhou, L. Wan, Z. Liang Sun, Structural elucidation of degradation products of olaquindox under stressed conditions by accurate mass measurements using electrospray ionization hybrid ion-trap/time-of-flight mass spectrometry, Int. J. Mass Spectrom. 303 (2011) 92–96.
[12] T. Yoshida, S. Mitsuhashi, Antibacterial activity of NM394, the active form of prodrug NM441, a new quinolone, Antimicrob. Agents Chemother. 37 (1993) 793–800.
[13] W. Jun, Z. Zhenyu, H. Zhanying, W. Yiwen, F. Yan, L. Mei, F. Guarang, W. Yutain, Determination of the active metabolite of prulifloxacin in human plasma by HPLC with fluorescence detection, Chromatographia 66 (2007) 37–41.
[14] S.J. Keam, C.M. Perry, Prulifloxacin, Drugs 64 (2004) 2221–2234.
[15] M.G. Matera, Pharmacologic characteristics of prulifloxacin, Pulm. Pharmacol. Ther. 19 (2006) 20–29.
[16] K. Tougou, A. Nakamura, S. Watanabe, Y. Okuyama, A. Morino, Paraoxonase has a major role in the hydrolysis of prulifloxacin (NM441), a prodrug of a new antibacterial agent, Drug Metab Dispos. 26 (1998) 355–359.
[17] Y. Okuyama, K. Momota, A. Morino, Pharmacokinetics of prulifloxacin. 1st communication: absorption, distribution and excretion in rats, dogs and monkeys after a single administration, Arzneimittelschung 47 (1997) 276–278.
[18] Z. Lingli, W. Jun, P. Yaju, L. Zhen, F. Guorong, W. Yutian, Determination of ulifloxacin, the active metabolite of Prulifloxacin, in human plasma by a 96-well format solid-phase extraction and capillary zone electrophoresis, J. Chromatogr. B Anal. Technol. Biomed. Life Sci. 872 (2008) 172–176.
[19] X.L. Wang, A.Y. Li, H.C. Zhao, L.P. Jin, Lanthanide sensitized chemiluminescences method of flow-injection for the determination of ulifloxacin and prulifloxacin, J. Anal. Chem. 64 (2009) 75–81.
[20] Y. Zhongju, W. Xiaoli, Q. Weidong, Z. Huichun, Capillary electrophoresis–chemiluminescences determination of norfloxacin and prulifloxacin, Anal. Chim. Acta 623 (2008) 231–237.
[21] A.P. Dewani, V.J. Daulatkar, B.B. Barik, A.V. Chandewar, S.K. Kanungo, A validated stability-indicating HPLC method for the determination of prulifloxacin in bulk and tablet dosage form, J. Pharm. Res. 3 (2010) 2574–2577.
[22] L. Guo, M. Qi, X. Jin, P. Wang, H. Zhao, Determination of the active metabolite of prulifloxacin in human plasma by liquid chromatography–tandem mass spectrometry, J. Chromatogr. B: Anal. Technol. Biomed. Life Sci. 832 (2006) 280–285.